

First mapping of monthly and diurnal climatology of Saharan dust layer height over the Atlantic Ocean from EPIC/DSCOVR in deep space

Zhendong Lu¹, Jun Wang^{1,2*}, Xi Chen², Jing Zeng², Yi Wang^{2,3}, Xiaoguang Xu⁴, Kenneth E. Christian^{5,6}, John E. Yorks⁵, Edward P. Nowottnick⁵, Jeffrey S. Reid⁷, Peng Xian⁷

¹Interdisciplinary Graduate Program in Informatics, The University of Iowa, Iowa City, IA, United States

²Department of Chemical and Biochemical Engineering, Center for Global and Regional Environmental Research and Iowa Technology Institute, The University of Iowa, Iowa City, IA, United States

³Now at Key Laboratory of Regional Ecology and Environmental Change, School of Geography and Information Engineering, China University of Geosciences, Wuhan, China

⁴GESTAR-II and Department of Physics, University of Maryland Baltimore County, Baltimore, MD, United States

⁵NASA Goddard Space Flight Center, Greenbelt, MD, United States

⁶Earth System Science Interdisciplinary Center, University of Maryland, College Park, MD, United States

⁷U.S. Naval Research Laboratory, Monterey, CA, United States

*Correspondence: Jun Wang (jun-wang-1@uiowa.edu)

Contents of this file

Description of EPIC AOD and AOC retrieval

Description of calculation of dust mass extinction efficiency for MERRA-2

Description of Figures S1-S6

Figures S1-S6

Introduction

This supplement includes the descriptions of EPIC aerosol optical depth (AOD) and aerosol optical centroid height (AOCH) retrieval, calculation of dust mass extinction efficiency for MERRA-2 and Figure S1-S6. Figure S1 shows the number of the valid retrievals for monthly EPIC AOCH climatology from 4 years (June 2015 – June 2019) of EPIC measurements. Figure S2 displays the monthly mapping of total AOD, dust optical depth and smoke optical depth in our domain calculated from 13 years (June 2006 – June 2019) of CALIOP level 3 product. Figure S3 is the scatter plot for comparing the domain-averaged monthly AOCH climatology from EPIC versus CALIOP and from MERRA-2 versus CALIOP. Figure S4 presents the monthly mapping of the MERRA-2 AOCH climatology. Figures S5 and S6 show the 3-hourly mapping of Saharan dust layer height in wet season (May - October) over tropical North Atlantic Ocean (TNAO) from MERRA-2 dataset and 6-hourly mapping of the counterpart from NAAPS-RA dataset.

Description of EPIC AOD and AOCH retrieval

The AOD is first determined using the two EPIC atmospheric window channels at 680 and 780 nm, and the AOCH is subsequently derived based on the ratios of two oxygen absorption bands to their neighboring continuum bands (764/780 and 688/680). Following Xu et al. (2017), the Saharan dust aerosol model was obtained from the climatology of AERONET data. We assumed that the aerosol vertical profile follows a quasi-Gaussian distribution (Spurr & Christi, 2014).

$$\tau(z) = C \frac{\exp(-h|z - H|)}{[1 + \exp(-h|z - H|)]^2} \quad (S1)$$

where C is determined by total AOD, and h is related to the half-width parameter η by $\eta = \frac{\ln(3+\sqrt{8})}{h}$. The half-width parameter is fixed at 1 km. The H retrieved from our algorithm represents the altitude where the maximum aerosol extinction coefficient is located, i.e., AOCH. The deviations of our retrieved AOCH from CALIOP counterparts are generally within 1 km. See Xu et al. (2017) for more details about the EPIC AOCH retrieval algorithm over ocean surface.

Description of calculation of dust mass extinction efficiency for MERRA-2

The aerosol extinction coefficient at vertical layer i from MERRA-2 $\beta_{\text{ext},i}$ for all 72 model layers is computed by Equation (S2).

$$\beta_{\text{ext},i} = \sum_{j=1}^m k_{ij} r_{ij} \rho_i \quad (\text{S2})$$

here k_{ij} is mass extinction efficiency of dust size bin j at vertical layer i ; r_{ij} is the mass mixing ratio of dust size bin j at vertical layer i from MERRA-2; and ρ_i is the air density at vertical layer i from MERRA-2. The mass extinction efficiency for 5 dust size bins is taken from the lookup tables of aerosol optical properties used in GEOS-4/5 (Colarco et al., 2010; Colarco et al., 2014), which is then linearly interpolated from 675 and 870 nm to the same wavelength of EPIC AOC retrieval at 680 nm.

Description of Figures S1-S6

Figure S1 in this document maps the number of the valid retrievals (sample density) for monthly EPIC AOC climatology over TNAO from 4 years (June 2015 – June 2019) of EPIC measurements. We calculated the monthly climatology of total AOD, dust optical depth and smoke optical depth over the domain of our interest using 13 years (June 2006 – June 2019) of CALIOP level 3 product. The results are shown in Figure S2. The scatter plot for comparing the domain-averaged monthly AOC climatology from EPIC versus CALIOP and from MERRA-2 versus CALIOP is presented in Figure S3. To match the overpass time of CALIOP, only the EPIC data from 14:00 to 16:59 UTC and MERRA-2 data at 15:00 UTC are used in this comparison. The correlation coefficient (R), root mean square error (RMSE) and mean bias error (MBE) are calculated and labeled in Figure S3. Figure S4 is the monthly mapping of Saharan dust layer height over TNAO from 4 years (June 2015 – June 2019) of MERRA-2 data. Figure S5 and S6 present the diurnal mapping of the dust AOC over the TNAO for the wet season (May - October) calculated from the multi-year (June 2015 – June 2019) average of MERRA-2 (Gelaro et al., 2017) and NAAPS-RA (Lynch et al., 2016) datasets, respectively. We only considered the model grid cells with AOD higher than 0.2 for the comparison with EPIC retrievals.

- Figure S1 shows the sample density map of monthly EPIC AOC climate.
- Figure S2 presents the monthly climate of total AOD, dust optical depth and smoke optical depth from CALIOP level 3 product.
- Figure S3 is the scatter plot for comparing the domain-averaged monthly EPIC AOC climate and the counterparts from CALIOP data.
- Figure S4 presents the monthly mapping of dust AOC from multi-year MERRA-2 data at 15:00 UTC.
- Figure S5 displays the 3-hourly mapping of dust AOC in daytime from the 3-hourly instantaneous MERRA-2 dataset.
- Figure S6 presents the 6-hourly mapping of dust AOC during the whole day from the NAAPS-RA reanalysis data.

Figures S1-S6

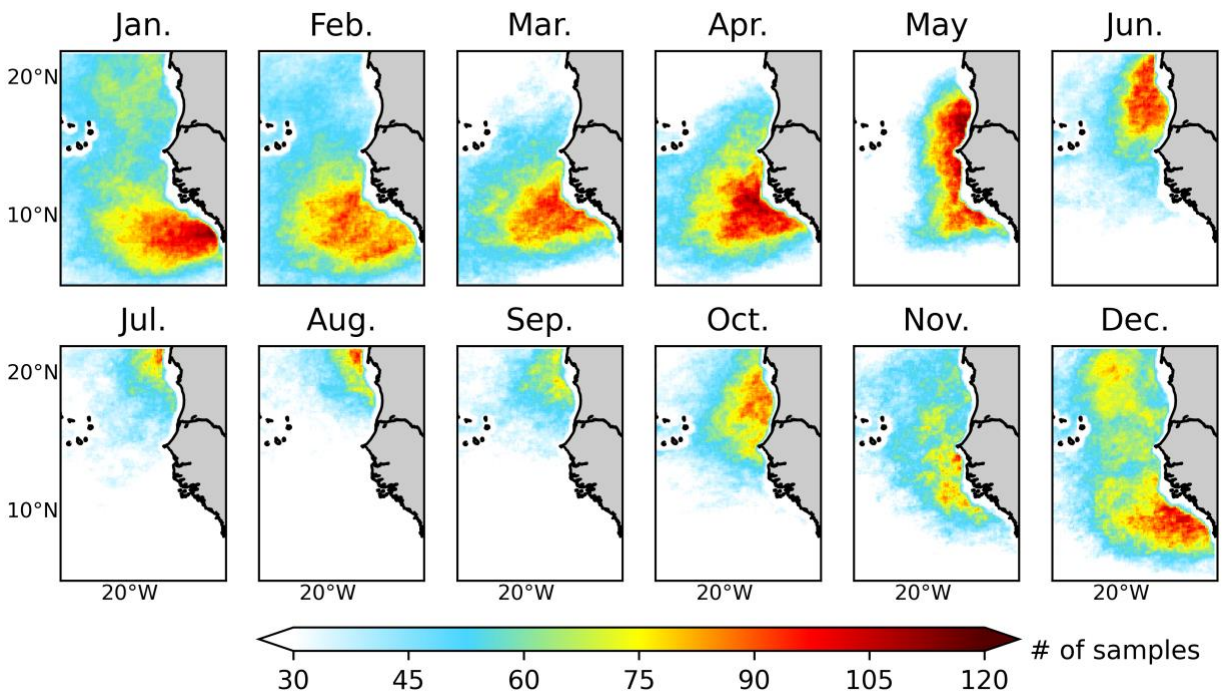


Figure S1. The number of valid retrievals for monthly EPIC AOC climate over TNAO from 4 years (June 2015 – June 2019) of EPIC measurements.

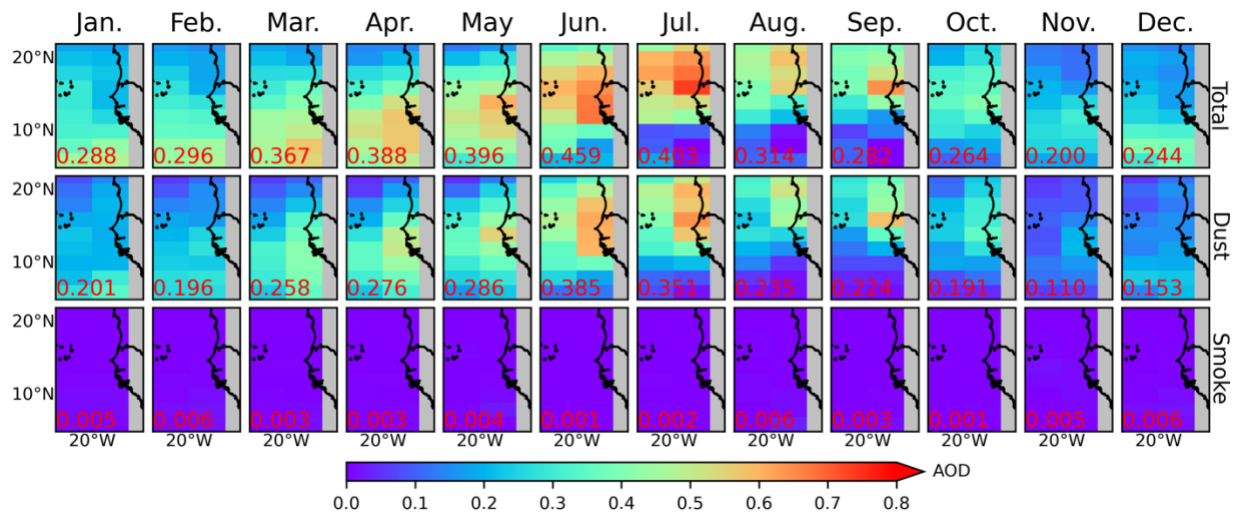


Figure S2. The monthly climatology of total AOD (top row), dust optical depth (middle row) and smoke optical depth (bottom row) over TNAO from 13 years (June 2006 – June 2019) of CALIOP level 3 product. The domain average is labeled by red font in each panel. The AOD values for dust and smoke are computed based on the CALIOP feature masks for different aerosol types. The AOD values for clean marine aerosols are not shown.

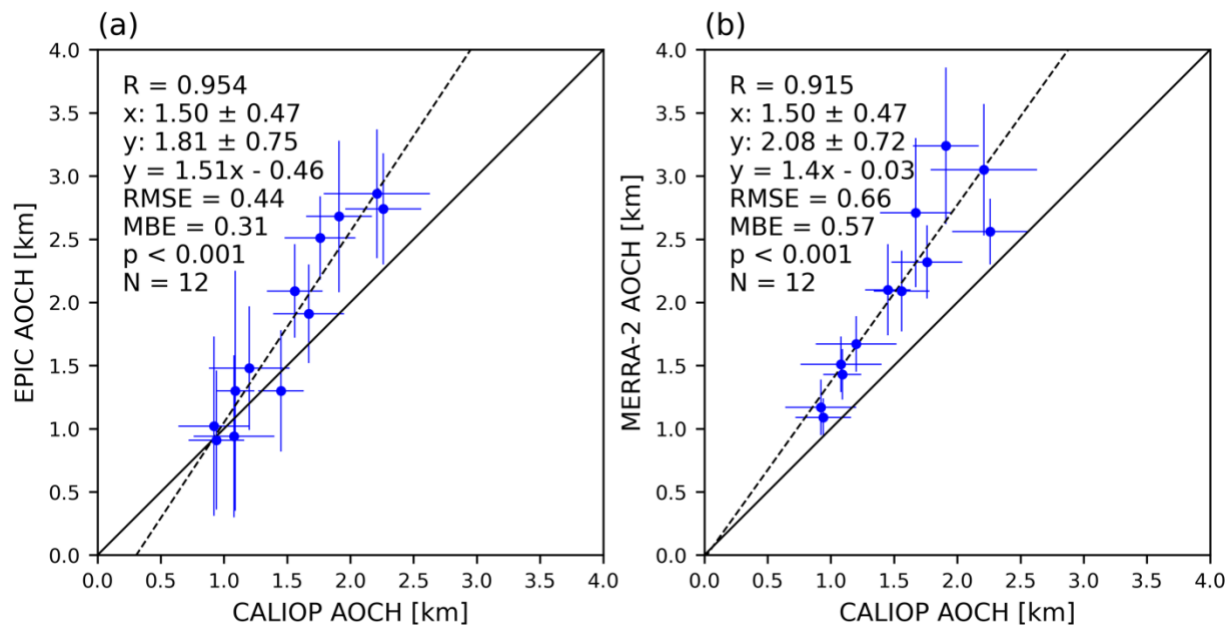


Figure S3. Scatter plot of monthly AOC climate from (a) EPIC versus CALIOP and (b) MERRA-2 versus CALIOP for 12 domain-averaged monthly data points. Only the EPIC data from 14:00 to 16:59 UTC and MERRA-2 data at 15:00 UTC were used to match the overpass time of CALIOP. The error bar represents the standard deviation of monthly AOC climate in the domain for each month. The correlation coefficient (R), mean and standard deviation of x and y axis, the fitted linear equation between x and y , root mean square error (RMSE) and mean bias error (MBE) are labeled in each panel.

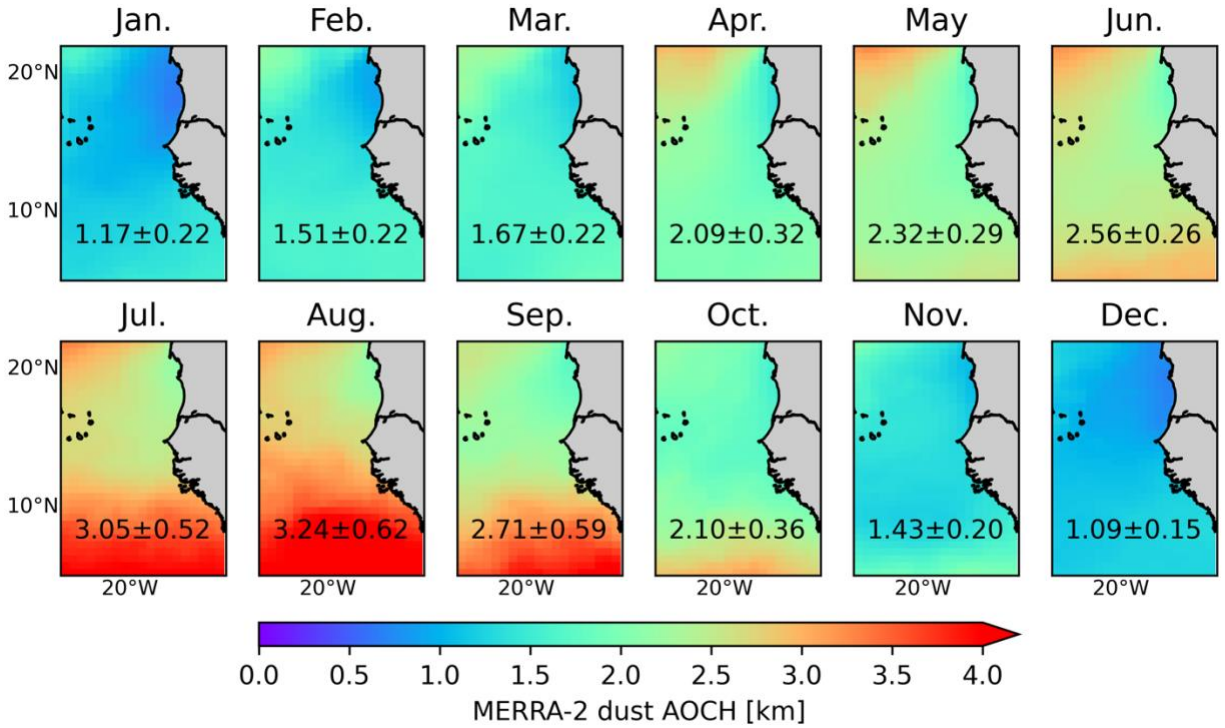


Figure S4. Monthly mapping of dust AOC over TNAO from MERRA-2 (June 2015 – June 2019). Only the data at 15:00 UTC were used to match the overpass time of CALIOP. The domain average \pm standard deviation for each month are labeled in each panel.

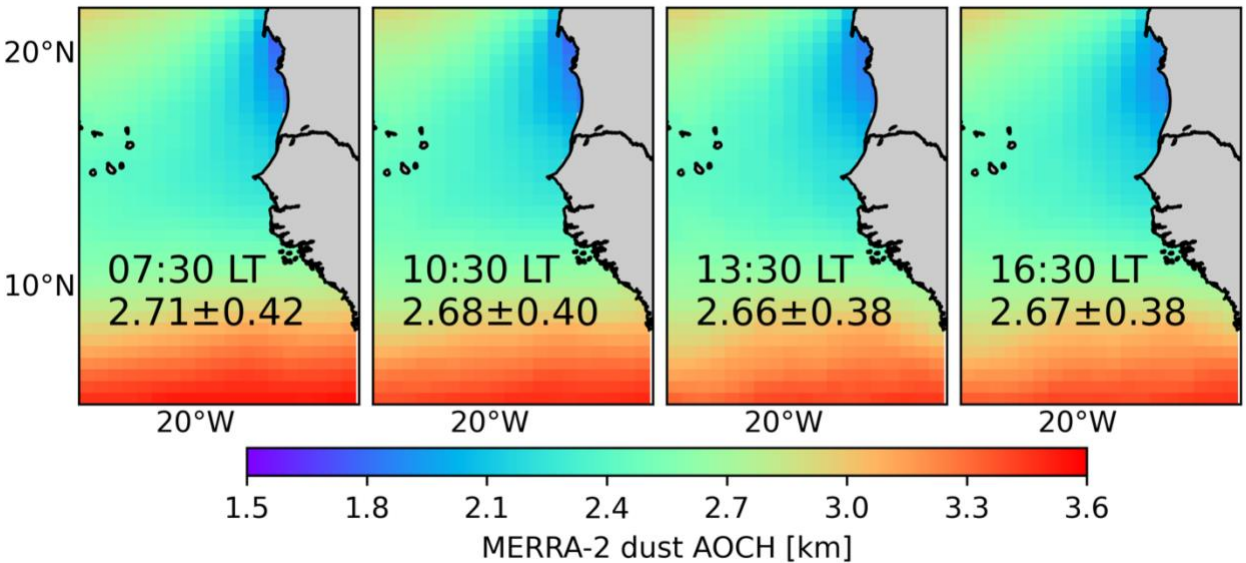


Figure S5. 3-hourly mapping of dust AOC over TNAO in wet season from MERRA-2 (June 2015 – June 2019). The local time (LT) and domain average \pm standard deviation are labeled in each panel.

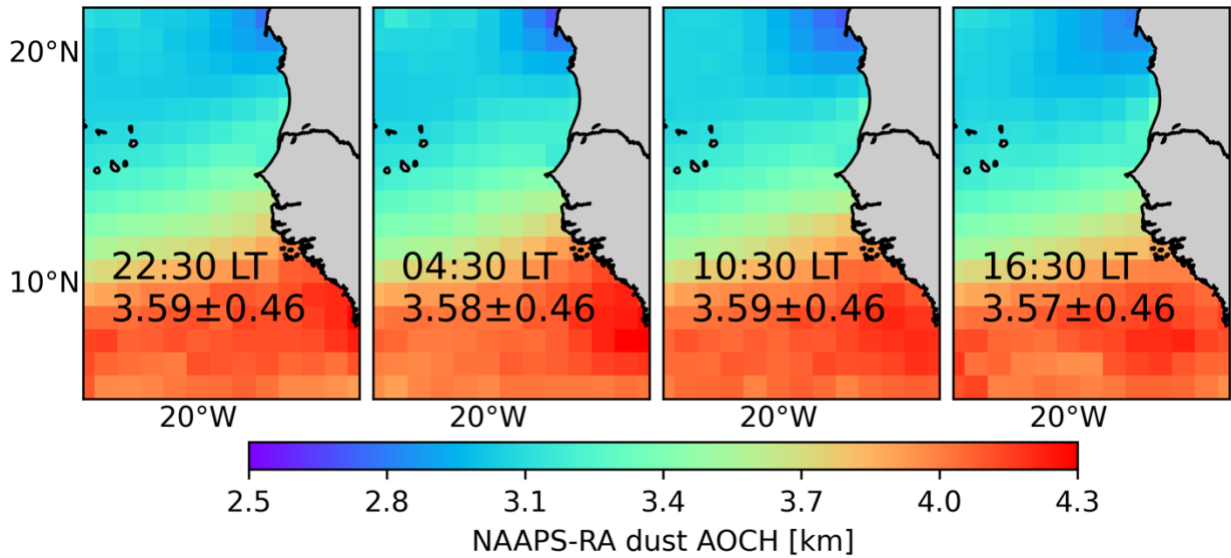


Figure S6. 6-hourly mapping of dust AOC over TNAO in wet season from NAAPS-RA (June 2015 – June 2019). The local time (LT) and domain average \pm standard deviation are labeled in each panel.

References

- Colarco, P. R., da Silva, A., Chin, M., & Diehl, T. (2010). Online simulations of global aerosol distributions in the NASA GEOS-4 model and comparisons to satellite and ground-based aerosol optical depth. *Journal of Geophysical Research-Atmospheres*, 115. 10.1029/2009jd012820
- Colarco, P. R., Nowottnick, E. P., Randles, C. A., Yi, B. Q., Yang, P., Kim, K. M., et al. (2014). Impact of radiatively interactive dust aerosols in the NASA GEOS-5 climate model: Sensitivity to dust particle shape and refractive index. *Journal of Geophysical Research-Atmospheres*, 119(2), 753-786. 10.1002/2013jd020046
- Gelaro, R., McCarty, W., Suarez, M. J., Todling, R., Molod, A., Takacs, L., et al. (2017). The Modern-Era Retrospective Analysis for Research and Applications, Version 2 (MERRA-2). *Journal of Climate*, 30(14), 5419-5454. 10.1175/jcli-d-16-0758.1
- Lynch, P., Reid, J. S., Westphal, D. L., Zhang, J. L., Hogan, T. F., Hyer, E. J., et al. (2016). An 11-year global gridded aerosol optical thickness reanalysis (v1.0) for atmospheric and climate sciences. *Geoscientific Model Development*, 9(4), 1489-1522. 10.5194/gmd-9-1489-2016
- Spurr, R., & Christi, M. (2014). On the generation of atmospheric property Jacobians from the (V)LIDORT linearized radiative transfer models. *Journal of Quantitative Spectroscopy & Radiative Transfer*, 142, 109-115. 10.1016/j.jqsrt.2014.03.011
- Xu, X., Wang, J., Wang, Y., Zeng, J., Torres, O., Yang, Y., et al. (2017). Passive remote sensing of altitude and optical depth of dust plumes using the oxygen A and B bands: first results from EPIC/DSCOVR at Lagrange-1 point. *Geophysical Research Letters*, 44(14), 7544-7554. 10.1002/2017gl073939